ARCHIVE OF MECHANICAL ENGINEERING

DOI: 10.24425/ame.2024.151331 2024, Vol. 71, No. 3, pp. 323–349

Ratiba FELLAG [1], Mahmoud BELHOCINE [1]

Comparative analysis of PID, fuzzy PID, and ANFIS controllers for 2-DOF helicopter trajectory tracking: simulation and hardware implementation

Received 1 May 2024, **Revised** 19 August 2024, **Accepted** 18 September 2024, **Published online** 23 September 2024

Keywords: ANFIS, fuzzy logic, helicopter, Quanser Aero 2, PID, matched disturbances

This study investigates advanced control techniques to evaluate the trajectory tracking control of a two-degrees-of-freedom (2-DOF) helicopter system based on simulation and hardware implementation experiments. For this, a Quanser Aero 2 platform and its QUARC software, integrated within MATLAB/Simulink, are used to design and implement multiple controllers, including Proportional Integral Derivative (PID), Fuzzy PID, and Adaptive Neuro Fuzzy Inference System (ANFIS) controllers. A two-phase approach was followed to assess and compare these controllers' ability to handle parametric uncertainties, unmodeled dynamics, and matched disturbances. Firstly, simulation experiments were conducted using an uncertain system model, considering the controller's responses in scenarios with and without cross-coupling and matched disturbances. Subsequently, hardware experiments were conducted under the same conditions to validate the simulation results, providing real-time performance comparisons. Finally, a rigorous quantitative assessment based on multiple performance metrics including Root Mean Square Error (RMSE), peak value, Integral Square Error (ISE), Integral of Absolute Error (IAE), and Integral of Time-multiplied Absolute Error (ITAE) demonstrated overperformance achieved using ANFIS for pitch control and Fuzzy PID for yaw control.

1. Introduction

Over recent years, there has been a significant surge in research focused on Unmanned Aerial Vehicles (UAVs), particularly concerning their control, stability, and tracking. From uses in defense and security sectors [1] to urban and remote

✉ Ratiba FELLAG, email: rfellag@cdta.dz

[1]Robotics and Industrial Automation Laboratory, Centre de Développement des Technologies Avancées (CDTA), Algiers, Algeria.

surveillance in cities or inaccessible locations [2], as well as applications in the agricultural industry involving aerial monitoring and spraying [3]. This surge in interest has led to advancements in the development and control of UAVs, which come in diverse configurations, including fixed-wing, multi-rotor, and helicopters. This latter stands out because it requires the fewest number of motors to achieve a stable flight, typically just two or three.

The helicopter system represents a complex, nonlinear plant with multiple variables. It incorporates electric actuators and rotary wings, all governed by a control system. This integrated setup generates the required thrust to counter aerodynamic drag during forward motion and the necessary lift force to support the helicopter's weight. The control design for such a system faces significant challenges due to the cross-coupling between inputs and outputs and the uncertainty surrounding the precise acquisition of the model's parameters and external disturbances [4, 5]. Consequently, there is a critical need for efficient control strategies to enhance the performance of the helicopter in achieving control tasks such as tracking and stabilization [6–8].

Traditional strategies to address the helicopter's motion control, such as Proportional Integral (PI) or Proportional Integral Derivative (PID) control [9], require linearization of the system to bring its control to specific operating points. However, this approach often conflicts with the nonlinear nature of the helicopter and the aforementioned disturbances and uncertainties. Moreover, tuning and adjusting PID parameters under such conditions can be challenging. Modern control is embracing new intelligent methods that emulate the essential characteristics of the human brain. These features include adapting and learning, planning under high uncertainty, and working with large amounts of data [10]. The well-known intelligent methods comprise neural networks, fuzzy logic, and hybrid systems combining more than one of the above techniques or classical control approaches [11].

Researchers have proposed various intelligent control approaches for two-degrees-of-freedom (2-DOF) helicopters in the literature, each offering distinct advantages and drawbacks. Some of these works include fuzzy logic [12], which provides a more intuitive and human-like approach to decision-making for complex dynamic systems. Fuzzy logic control has proven to be effective for controlling the 2-DOF helicopter [13, 14]. This control method adapts to changes in operating conditions and uncertainties, leading to better tracking performance, reduced overshoot, and enhanced stability. This efficacy makes fuzzy logic a valuable tool for combining with other approaches, such as PID [15], Linear quadratic regulator (LQR) [16], and sliding mode control [17–20], to exploit their respective strengths. Fuzzy PID control combines the adaptive and flexible nature of fuzzy logic with the precision and stability of PID control [21, 22]. Unlike conventional PID controllers that rely on fixed, pre-defined parameters, a fuzzy PID controller incorporates linguistic rules and membership functions to

adapt the gains to changing conditions and uncertainties based on real-time system behavior.

Another intriguing fusion for controlling 2-DOF helicopters involves Neuro-Fuzzy control [23–25]. This hybrid approach integrates the adaptability of fuzzy logic with the learning capabilities of neural networks both contributing to improved tracking and overall system performance. A particular type of neuro-fuzzy control is the Adaptive Network-based Fuzzy Inference System (ANFIS) [26]. The key feature of ANFIS is its systematic layered architecture. It uses a hybrid learning algorithm to adjust parameters based on both input-output data and predefined fuzzy rules. The resulting ANFIS model can adapt to changing conditions and learn from experience, making it particularly effective for control applications where a combination of fuzzy logic and neural network capabilities is beneficial. In [27], an online ANFIS controller is used for a 2-DOF helicopter.

Inspired by the discussion above, each method contributes to advancing control systems, addressing specific challenges, and offering unique benefits and limitations.This study aims to provide a comprehensive evaluation and comparison of three controllers, namely PID, Fuzzy PID, and ANFIS, for robust trajectory tracking of the Quanser Aero 2 2-DOF helicopter system under parametric uncertainties, unmodeled dynamics, cross-coupling, matched disturbances, and input saturation. The novelty of this work lies in the systematic investigation of these controllers' performance through both simulation and real-time hardware implementation, considering a range of uncertainties and disturbances that are commonly encountered in practical UAV applications. A rigorous quantitative assessment based on multiple performance metrics including Root Mean Square Error (RMSE), peak value, Integral Square Error (ISE), Integral of Absolute Error (IAE), and Integral of Time-multiplied Absolute Error (ITAE) is presented to evaluate the controller's efficacy. Moreover, by utilizing the capabilities of the QUARC software and the Quanser Aero 2 platform [28], integrated with MATLAB/Simulink, this study offers insights into the most effective control strategy for achieving robust trajectory tracking under challenging conditions. The findings of this study will contribute to the development of reliable and robust control systems for UAVs, enabling their safe and efficient operation in challenging real-world conditions.

The organization of this paper is the following. In section 2 we present the 2-DOF helicopter system description and modeling. In section 3 we detail the design procedures for the PID, Fuzzy PID, and ANFIS controllers. Section 4 covers the numerical simulations, evaluating the controllers' performance under uncertainties and disturbances. Section 5 presents the real-time hardware implementation results, where the controllers are tested on the Quanser Aero 2 platform. In section 6, we discuss and analyze the findings from both the simulation and hardware implementation experiments. Finally, section 7 concludes the paper and suggests future work directions.

2. System Description and Modeling

The Quanser Aero 2, depicted in Fig. 1 [29], is a reconfigurable dual-rotor laboratory experiment specifically designed by Quanser to perform aerospace control experiments. It can be arranged in a 2-DOF helicopter-like setup with the main thruster horizontally positioned and the tail thruster vertically, both powered by DC motors. The Quanser Aero 2 consists of a grounded base with a built-in data acquisition card, a set of encoders to measure angular positions of pitch and yaw axes, and an Inertial Measurement Unit (IMU).

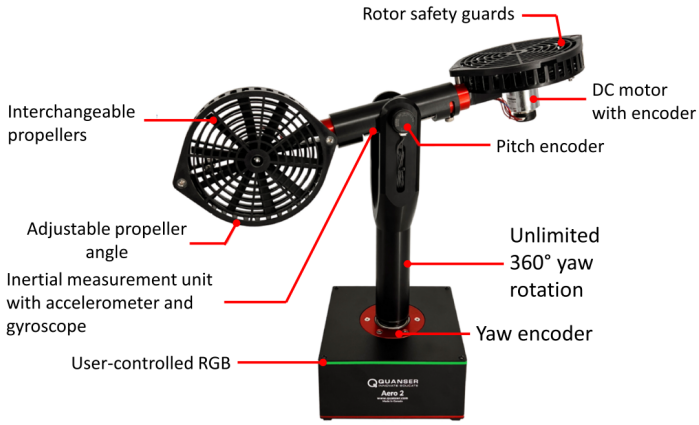

Fig. 1. Quanser Aero 2 [29]

From a control perspective, the 2-DOF helicopter configuration represents a higher-order nonlinear MIMO (Multiple Input Multiple Output) system characterized by prominent cross-couplings between pitch and yaw axes. The free body diagram, illustrated in Fig. 2, allows us to obtain the following equations of motion about the horizontal axis [30] for the pitch and yaw axes, respectively:

$$\begin{aligned} J_p\ddot{\theta} + D_p\dot{\theta} + K_{sp}\theta &= \tau_p, \\ J_y\ddot{\psi} + D_y\dot{\psi} &= \tau_y, \end{aligned} \tag{1}$$

where the forces exerted on the pitch and yaw axes are:

$$\begin{aligned} \tau_p &= K_{pp}D_tV_p + K_{py}D_tV_y, \\ \tau_y &= K_{yp}D_tV_p + K_{yy}D_tV_y. \end{aligned} \tag{2}$$

The physical parameters used in equations (1) and (2) are described in Table. 1. Some of the model parameters are provided in the Quanser Aero 2 user manual [30], while the remaining ones are determined through experimental identification. These latter cannot be precisely accurate, implying the presence of uncertainties

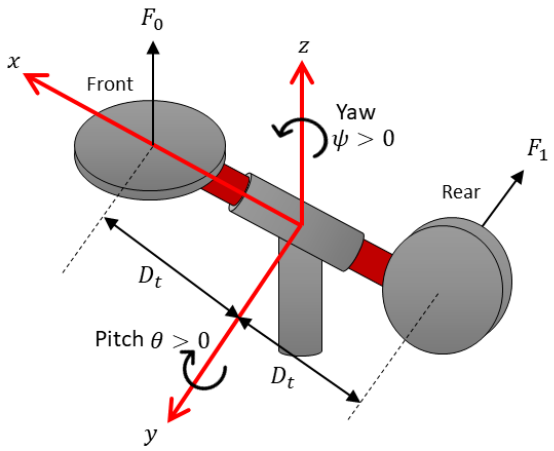

Fig. 2. Free body diagram of the Quanser Aero 2 [30]

Table 1. Physical parameters of the Quanser Aero 2 helicopter [31]

Symbol	Description	Value	Unit
J_p	Pitch axis inertia	0.0232	Kg m^2
J_y	Yaw axis inertia	0.0238	Kg m^2
D_p	Pitch axis damping	0.0020	Nm/V
D_y	Yaw axis damping	0.0019	Nm/V
K_{sp}	Pitch axis stiffness	0.0074	Nm/V
K_{pp}	Pitch thrust gain from front rotor	0.0032	N/V
K_{py}	Pitch thrust gain from rear rotor	0.0014	N/V
K_{yy}	Yaw thrust gain from rear rotor	0.0061	N/V
K_{yp}	Yaw thrust gain from front rotor	-0.0032	N/V
D_t	Distance between pivot and rotor center	0.1674	m

in the helicopter model. On the other hand, we notice from eq. (2) that a reaction torque is acting from the pitch axis to the yaw axis and vice-versa, which implies cross-coupling between axes.

Considering initial conditions to be null and using the Laplace transform, the following transfer functions (3) are derived to describe the system motions to voltage inputs for the pitch and yaw axes, respectively.

$$\begin{aligned} \Theta(s) &= G_{11}(s)V_p(s) + G_{12}(s)V_y(s), \\ \Psi(s) &= G_{21}(s)V_p(s) + G_{22}(s)V_y(s), \end{aligned} \tag{3}$$

with the transfer function $G_{11}(s)$, $G_{12}(s)$, $G_{21}(s)$ and $G_{22}(s)$ which are defined as:

$$
\begin{aligned}
G_{11}(s) &= \frac{K_{pp}D_t}{J_p s^2 + D_p s + K_{sp}},\\
G_{12}(s) &= \frac{K_{py}D_t}{J_y s^2 + D_y s},\\
G_{21}(s) &= \frac{K_{yp}D_t}{J_p s^2 + D_p s + K_{sp}},\\
G_{22}(s) &= \frac{K_{yy}D_t}{J_y s^2 + D_y s}.
\end{aligned} \tag{4}
$$

3. Controllers Design

In this section, the basic concepts behind the design of the PID, Fuzzy PID and ANFIS controllers will be introduced for the specific application of the trajectory tracking of Quanser Aero 2.

3.1. PID controller

The PID controller stands as a widely adopted and favored control method across various industries. The fundamental concept behind the PID controller lies in computing the difference between the desired value, denoted as $r(t)$, and the real-time measured output, denoted as $y(t)$, then continuously monitoring this difference to steer systems' output towards the desired setpoint:

$$er(t) = r(t) - y(t). \tag{5}$$

The typical control law for a PID controller using eq. (5) is:

$$u = k_p\,(er(t)) + k_d\left(\frac{\mathrm{d}}{\mathrm{d}t}er(t)\right) + k_i\left(\int er(t)\,\mathrm{d}t\right), \tag{6}$$

where k_p is the proportional gain, k_d is the derivative gain, and k_i is the integral gain.

In this work, two PID controllers are designed to regulate the motion of the pitch and yaw axes of the Quanser Aero 2 helicopter to desired positions, respectively, using eqs. (3) and (4). Hence, for the pitch axis, $r\,(t) = \theta_d(t)$ is the reference pitch angle, and $y\,(t) = \theta(t)$ is the measured pitch angle, and $u = V_p$ the control input, which represents the applied motor voltage to the front pitch rotor. For the case of yaw axis control, $r\,(t) = \psi_d(t)$ is the desired yaw angle, $y\,(t) = \psi(t)$ the measured yaw angle and the control input of the rear yaw rotor motor is the voltage $u = V_y$.

The PID controller's gains were adjusted manually during simulations using the Ziegler-Nichols tuning method to determine the most suitable values for the three PID parameters corresponding to the best regulation outcome of the pitch and yaw angles.

3.2. Fuzzy PID controller

Unlike conventional logic, fuzzy logic, introduced by Zadeh in 1965 [12], uses linguistic variables to emulate the human mind. This type of processing, although simple, is remarkably powerful and closely aligns with human expert reasoning. Mathematically, a fuzzy controller employs control laws that incorporate IF $\cdots$ THEN logical rules, combined with fuzzy membership functions to effectively regulate the process and minimize errors.

This work presents a methodology for integrating the error between desired and actual output trajectories, as well as its time derivative from the input PID regulator into a fuzzy controller. To achieve this, the parameters k_p, k_i, and k_d are written as nonlinear fuzzy functions and independently adjusted using three distinct fuzzy controllers, as illustrated in Fig. 3.

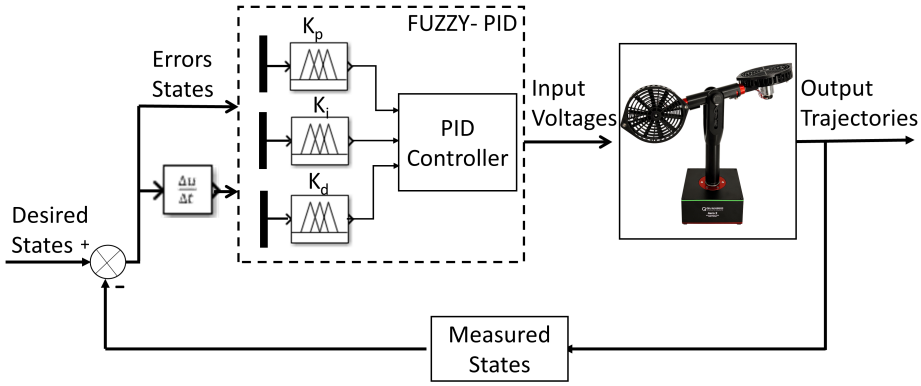

Fig. 3. Fuzzy PID controller

The fuzzy logic systems were created utilizing the Mamdani inference method and integrated into the PID regulator for real-time turning of its gains. The corresponding fuzzy rules, enumerated in Table. 2, Table. 3 and Table. 4 show the mapping of input and the output linguistic variables for the (k_p), (k_i) and (k_d) gains, respectively. Five fuzzy sets, represented by triangular membership functions, are used to represent the input variables (error and its rate of change). These fuzzy sets are labeled as NB (Negative Big), N (Negative), ZE (Zero), P (Positive), and PB (Positive Big). Similarly, triangular membership functions are employed to represent the output variables, namely the PID controller's gains k_p, k_i, and k_d. These fuzzy sets are labeled as S (Small), MS (Medium Small), MB (Medium Big), and B (Big). The center of gravity method is employed for defuzzification to determine the final output value of the fuzzy system. This method is chosen due to its ability to achieve high control sensitivity to changes in the input signals while maintaining computational efficiency, making it suitable for real-time control applications.

Finally, two Fuzzy PID controllers are implemented within MATLAB/Simulink to control the motion of the pitch and yaw axes of the 2-DOF helicopter: Quanser Aero 2.

Table 2. Fuzzy rule base for k_p

e \ de	NB	N	ZE	P	PB
NB	**B**	**B**	**MB**	**S**	**MS**
N	**B**	**MB**	**MS**	**S**	**S**
ZE	**MB**	**MS**	**S**	**MS**	**MB**
P	**S**	**S**	**MS**	**MB**	**B**
PB	**MS**	**S**	**MB**	**B**	**B**

Table 3. Fuzzy rule base for k_i

e \ de	NB	N	ZE	P	PB
NB	**MB**	**MS**	**S**	**MS**	**MB**
N	**B**	**MB**	**MS**	**MB**	**B**
ZE	**B**	**MB**	**S**	**MB**	**B**
P	**B**	**MB**	**MS**	**MB**	**B**
PB	**MB**	**MS**	**S**	**MS**	**MB**

Table 4. Fuzzy rule base for k_d

e \ de	NB	N	ZE	P	PB
NB	**S**	**S**	**MS**	**S**	**S**
N	**MB**	**MS**	**MS**	**MS**	**MB**
ZE	**B**	**MS**	**S**	**MS**	**B**
P	**MB**	**MS**	**MS**	**MS**	**MB**
PB	**S**	**S**	**MS**	**S**	**S**

3.3. ANFIS controller

The ANFIS (Adaptive Neuro Fuzzy Inference System) controller represents an advanced fusion of Fuzzy Logic with an Artificial Neural Network (ANN), employing neuro-adaptive learning methods to dynamically construct membership functions (MF) and control rules [26]. The ANFIS consists of a five-layer architecture utilized for model development [32, 33], as illustrated in Fig. 4.

ANFIS is based on the Takagi–Sugeno fuzzy inference system and is considered a universal estimator. The training and validation data are derived from the

closed-loop output results obtained using the conventional PID controller. Subsequently, the model is trained using the hybrid optimization training algorithm proposed by MATLAB [34], and its performance is evaluated by comparing it to the experimental data obtained from the output results of the PID controller. The ANFIS model is generated using the MATLAB toolbox "Neuro-Fuzzy Designer," offering a robust framework for various tasks, as depicted in Fig. 5.

Designing an ANFIS controller for the 2-DOF helicopter system involves employing the error and its derivative as inputs. Fig. 4 and Fig. 5 illustrate the various layers of the controller, which are described further below.

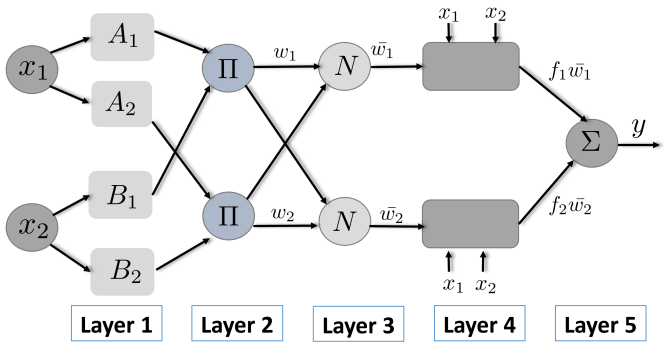

Fig. 4. 5-Layer ANFIS structure

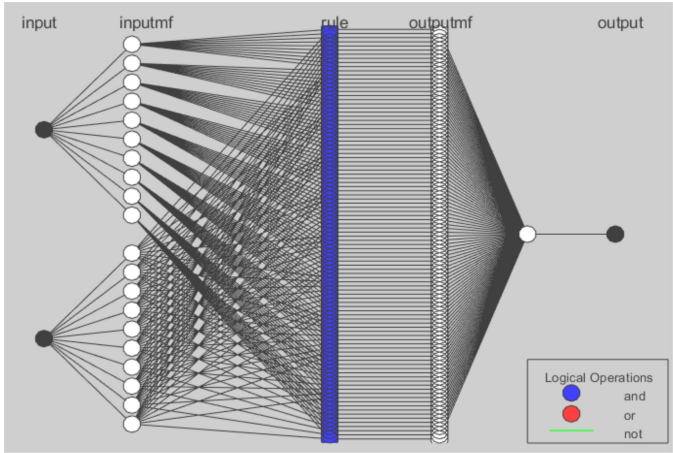

Fig. 5. Structure of ANFIS within MATLAB/Simulink [34]

3.3.1. First layer: Fuzzification layer

In this layer, the fuzzification takes place. This means that each non-fuzzy entry is assigned a membership value for each fuzzy subset. Gaussian membership

functions represented in (7) have been selected for each entry [33]. This layer consists of nodes, and each node is an adaptive node.

$$\mu_{A_i}(x) = \exp\left[-\left(\left(\frac{x - c_i}{a_i}\right)^2\right)^{b_i}\right], \quad \text{for } i = 1, 2, \tag{7}$$

where c_i is the center (mean) of the Gaussian curve, a_i is the curve's width, and b_i is the premise parameter.

3.3.2. Second layer: Rules layer

The output of each fixed node in this layer, shown by the symbol Pi, is the sum of all incoming signals:

$$O_{2,i} = \omega_i = \mu_{A_i}(x) \times \mu_{B_i}(x), \quad \text{for } i = 1, 2. \tag{8}$$

The output of each node $O_{2,i}$ represents the trigger intensity of a rule [32], and ω_i is the firing strength of the i^{th}-rule.

3.3.3. Third layer: Normalization layer

Each fixed node in this layer is labeled as N. The i^{th}-estimate node is in charge of calculating the relationship between the trigger intensity of the i^{th}-estimate and the fuzzy rule with respect to the sum of their trigger intensities.

$$O_{3,i} = \bar{\omega}_i = \frac{\omega_i}{\omega_1 + \omega_2}, \quad \text{for } i = 1, 2. \tag{9}$$

For convenience, each output of this layer is referred to as the normalized trigger intensity [32].

3.3.4. Fourth layer: Defuzzification layer

Each node i belonging to this layer is called an adaptive node and is determined as follows:

$$O_{4,i} = \bar{\omega}_i f_i = \bar{\omega}_i \left(p_i x + q_i y + r_i\right), \quad \text{for } i = 1, 2. \tag{10}$$

where $\bar{\omega}_i$ is the normalized trigger intensity from the third layer and p_i, q_i, r_i are the set of parameters known as consequent parameters [32] of the ANFIS algorithm and are adjusted using recursive least squares algorithm.

3.3.5. Fifth layer: Output Layer

The node in this layer is called Σ, because it summates all the incoming signals as $O_{5,i}$ to obtain an adaptive network that is functionally similar to a Sugeno fuzzy model.

$$O_{5,i} = \sum_i \bar{\omega}_i f_i = \frac{\sum_i \omega_i f_i}{\sum_i \omega_i}, \qquad \text{for } i = 1, 2. \tag{11}$$

4. Simulation Results

Before implementing the controllers on the Quanser Aero 2 platform, we proceed first at simulating the PID, fuzzy PID, and ANFIS controllers using the developed uncertain model expressed by eq. (3) within MATLAB/Simulink. The simulation experiments involve two cases, first by considering a decoupled undisturbed model, then by introducing cross-coupling and reaction torques along with non-vanishing matched disturbances provided by a band-limited white noise to assess the robustness of the controllers.

The desired trajectory for the pitch angle is selected as a square wave with an amplitude of 15° and a frequency of 0.05 Hz, while for the yaw angle, the input signal is a square wave with an amplitude of 30° and a frequency of 0.04 Hz. It should be noted that the input voltage of the 2-DOF Quanser Aero 2 helicopter platform is saturated by $Vp, Vy \in [-24,\ 24]\ V$. Initial conditions are considered null for both pitch and yaw angles. It should be mentioned that this saturation also affects the control input signals.

The values of $k_p = 116.3$, $k_i = 12.7$, and $k_d = 99.6$ are selected for the PID controller of the pitch motion. Whereas for the yaw motion, the values of PID gains are $k_p = 38.1$, $k_i = 5.3$ and $k_d = 34.5$, respectively. This choice is determined from the observation of the numerical simulations.

The following figures compare the desired trajectories (solid lines) to the measured trajectories using PID (dotted lines), Fuzzy PID (dashed lines) and ANFIS (Dash-dotted lines) for both axes (subfigures (a)). Additionally, the tracking errors between the desired and actual signals are displayed in subfigures (b).

4.1. Case 1: Decoupled undisturbed model

In this case, the dynamic model of the Quanser Aero 2 helicopter is simplified by assuming null transfer functions $G_{12}(s)$ and $G_{21}(s)$. While this model is acknowledged to be uncertain due to experimentally identified parameters, it does not include cross-coupling between axes.

In Fig. 6, we observe that all three controllers effectively track the desired pitch angle trajectory. However, the Fuzzy PID controller exhibits a smaller overshoot and a slightly slower convergence to the desired trajectory compared to the ANFIS

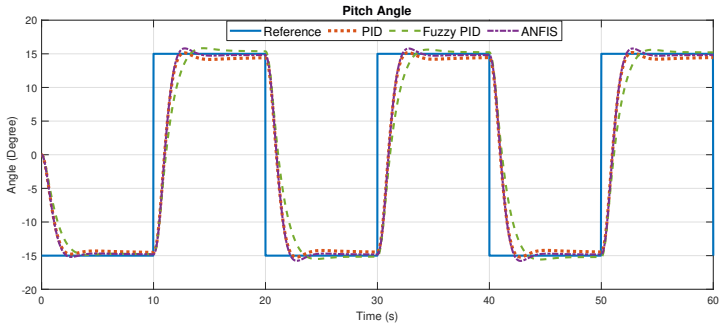

(a) Pitch trajectory tracking result

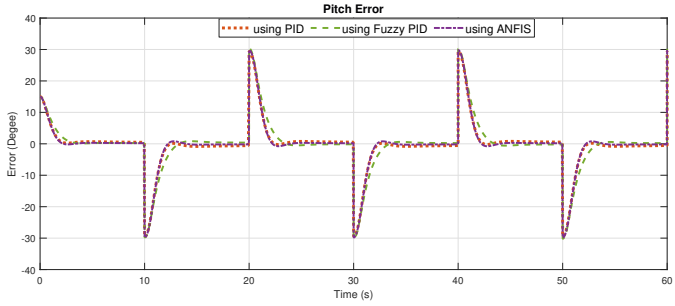

(b) Tracking error for pitch

Fig. 6. Simulation of trajectory tracking of pitch angle: undisturbed system

and PID controllers. This observation suggests that the Fuzzy PID controller may be more conservative in its control actions. The ANFIS controller, on the other hand, demonstrates a rapid and accurate response to the pitch angle trajectory. This is due to the ANFIS controller's ability to learn complex nonlinear relationships between the input and output signals. Overall, the ANFIS controller exhibits superior tracking performance for the pitch axis.

As illustrated in Fig. 7, all three controllers exhibit similar tracking performance for the yaw axis. While a slight overshoot is observed for the Fuzzy PID controller, the overall tracking accuracy is comparable to the ANFIS and PID controllers. This implies that the yaw motion appears to be less sensitive to controller differences compared to the pitch motion.

Fig. 8 and Fig. 9 depict the control inputs applied to the pitch and yaw propellers, respectively, by the ANFIS, Fuzzy PID, and PID controllers. In Fig. 8, it is observed that the ANFIS and PID controllers exhibit similar control input magnitudes for pitch motion. However, the Fuzzy PID controller consistently employs smaller control inputs.

In contrast to pitch motion, Fig. 9 demonstrates that the Fuzzy PID controller requires the largest control inputs for the yaw motion. The ANFIS and PID controllers, on the other hand, exhibit similar control input magnitudes.

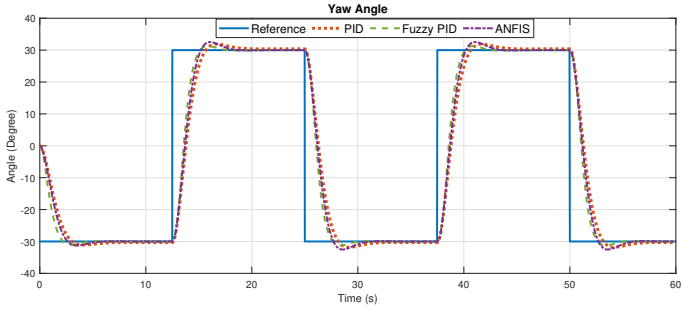

(a) Yaw trajectory tracking result

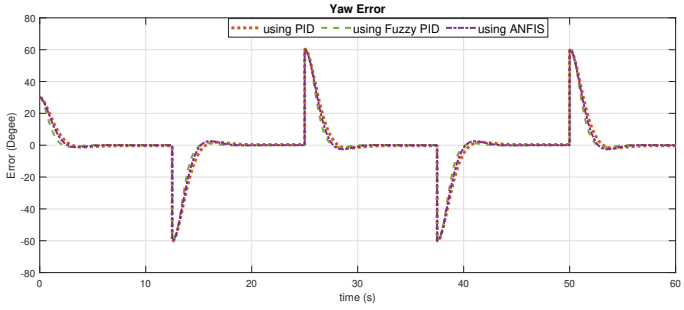

(b) Tracking error for yaw

Fig. 7. Simulation of trajectory tracking of yaw angle: undisturbed system

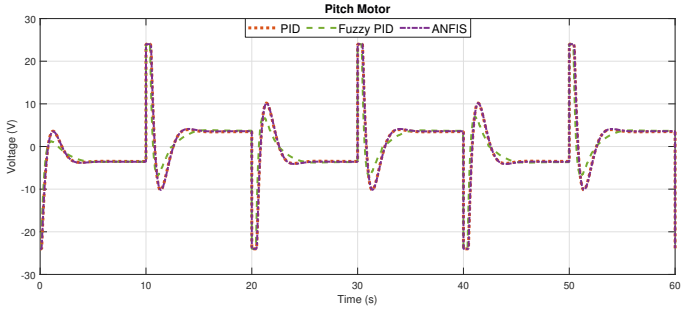

Fig. 8. Control performance in simulation: pitch angle without disturbance

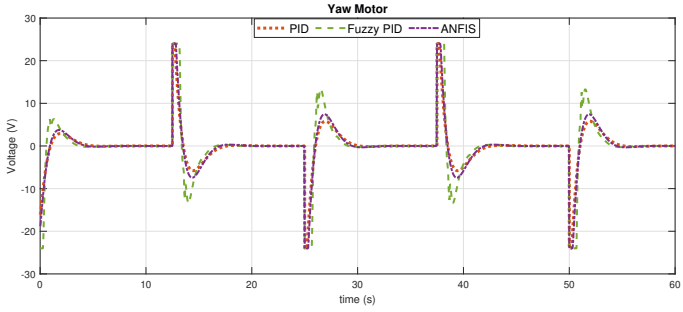

Fig. 9. Control performance in simulation: yaw angle without disturbance

It is noticed that the control signals of all three controllers reach the saturation level; however, each controller effectively accomplishes the trajectory tracking task.

4.2. Case 2: Coupled model with matched disturbances

To evaluate the controllers' robustness against cross-coupling and matched disturbances, we employ the comprehensive uncertain dynamic model outlined in equations (3) and (4). We introduce a non-vanishing band-limited white noise using a block that generates normally distributed random numbers, suitable for integration into continuous or hybrid systems. The generated noise signals are added to the input controls as matched disturbances. The initial conditions, desired trajectories, and controller parameters remain the same as in the previous simulation setup. The simulation results for both the pitch and yaw axes are illustrated in Figs. 10, 11, 12, and 13, respectively.

Fig. 10 and Fig. 11 show the effect of matched disturbances on the tracking responses. These figures demonstrate that all three controllers maintain effective tracking of the desired pitch and yaw trajectories despite the introduced noise disturbances and cross-coupling but with more overshoot. The ANFIS controller exhibits the most precise tracking for the pitch angle, followed by the Fuzzy PID

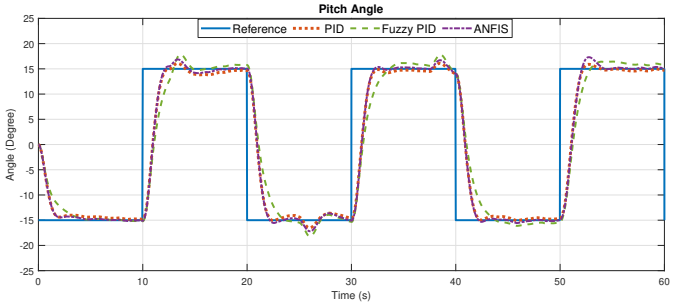

(a) Pitch trajectory tracking result

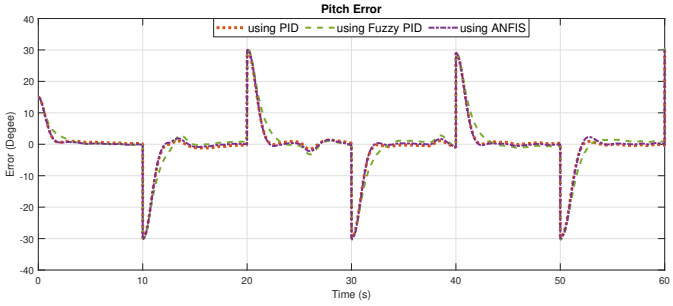

(b) Pitch tracking error result

Fig. 10. Simulation of pitch trajectory tracking with matched disturbance

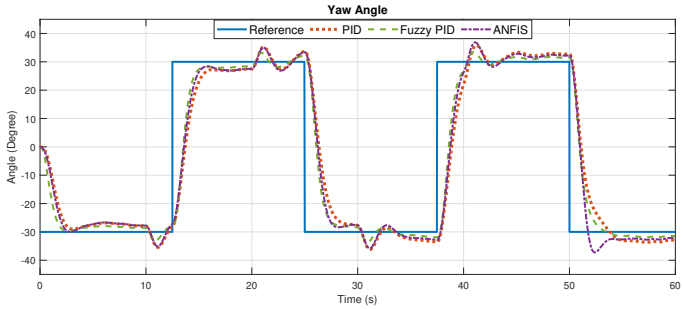

(a) Yaw trajectory tracking result

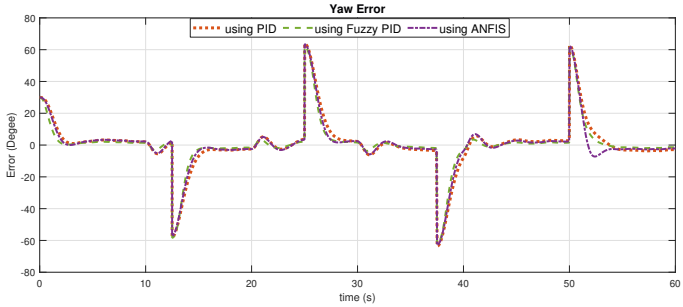

(b) Yaw tracking error result.

Fig. 11. Simulation of yaw trajectory tracking with matched disturbance

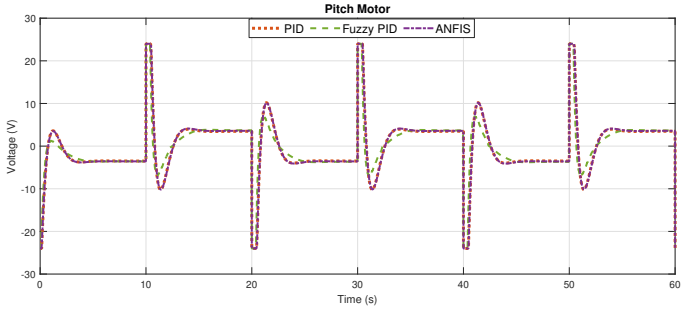

Fig. 12. Control performance of pitch angle in simulation under matched disturbance

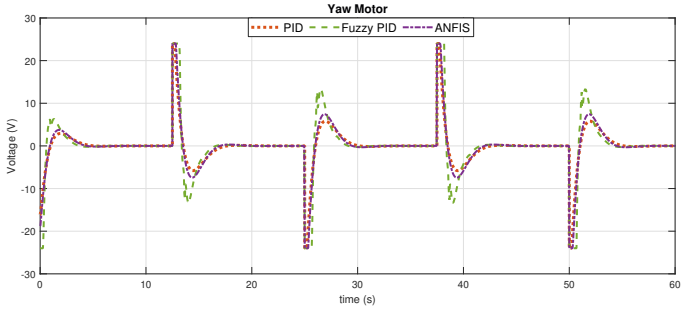

Fig. 13. Control performance of yaw angle in simulation yaw under matched disturbance

and PID controllers. In contrast, the Fuzzy PID is more accurate for the yaw angle tracking.

Regarding input control signals, Fig. 12 and Fig. 13 show that the control inputs for the pitch and yaw axes exhibit significant noise attributed to the non-vanishing band-limited white noise. Nevertheless, the obtained tracking responses show the robustness of the controllers to reject matched disturbances and to handle cross-coupling between pitch and yaw axes.

4.3. Comparison of simulation results

To quantitatively assess the performance of the PID, Fuzzy PID, and ANFIS controllers from the simulation viewpoint, we investigate five performance metrics: RMSE, peak value, ISE, IAE, and ITAE. RMSE is a common performance metric used in trajectory tracking tasks to measure the accuracy of a model or system in predicting or following a desired trajectory. It essentially measures the average distance between the desired and the actual trajectories. Smaller RMSE values indicate better tracking performance. Peak value, on the other hand, measures the maximum deviation by which the system's response exceeds the desired trajectory. A higher peak value indicates a more pronounced overshoot, while a lower peak value implies a smoother transition towards the desired trajectory. Finally, ISE, IAE and ITAE are commonly used performance metrics in trajectory tracking tasks. They measure the cumulative error between the desired and actual trajectories over time. Smaller metrics values indicate better tracking performance, implying that the system consistently follows the desired trajectory with minimal deviations.

Table 5 and Table 6 indicate calculated performance metrics from the simulation results of applying PID, Fuzzy PID, and ANFIS to track pitch and yaw trajectories of the Quanser Aero 2 helicopter system for both cases with and without disturbances. Analyzing the pitch motion, the three controllers achieve satisfactory tracking performance without disturbances. However, when disturbances are introduced, the ANFIS controller demonstrates the lowest RMSE, ISE, IAE, and ITAE values, indicating better tracking accuracy and minimizing overall error accumulation. In terms of peak value, the PID controller shows the lowest values in both cases. Despite disturbances, all three controllers can effectively limit overshoot and maintain smooth transitions toward the desired trajectory.

Table 5. Simulation comparison for pitch axis

	Without disturbance			Disturbed model		
Metric	PID	Fuzzy PID	ANFIS	PID	Fuzzy PID	ANFIS
RMSE	8.210	7.643	**7.577**	7.641	8.226	**7.561**
Peak Value (°)	**15.19**	15.73	15.80	**16.10**	17.85	17.31
ISE ($\times 10^4$)	0.354	0.404	**0.350**	0.362	0.406	**0.351**
IAE ($\times 10^4$)	195.1	224.3	**180.9**	189.1	240.3	**185.2**
ITAE ($\times 10^4$)	0.560	0.640	**0.513**	0.626	0.662	**0.546**

Table 6. Simulation comparison for yaw axis

	Without disturbance			Disturbed model		
Metric	PID	Fuzzy PID	ANFIS	PID	Fuzzy PID	ANFIS
RMSE	15.70	**14.41**	15.09	17.85	**16.17**	17.31
Peak Value (°)	31.89	**31.30**	32.53	35.84	**33.44**	36.87
ISE ($\times 10^4$)	1.479	**1.246**	1.366	1.568	**1.364**	1.408
IAE ($\times 10^4$)	400.8	**311.6**	357.7	499.6	**376.5**	446.6
ITAE ($\times 10^4$)	1.162	**0.906**	1.034	1.461	**1.094**	1.293

In contrast, the Fuzzy PID controller presents the lowest RMSE, RMSE, ISE, IAE, and ITAE values for the yaw motion under both conditions, indicating better tracking accuracy and minimizing overall error accumulation. It also shows the smallest peak value among the three controllers. This indicates that the Fuzzy PID controller can effectively limit overshoots. In this context, the Fuzzy PID emerges as the most effective controller for the yaw axis. These results support and affirm the observations made from trajectory tracking graphs presented earlier.

5. Real-time implementation results

A real-time control system has been implemented on the Quanser Aero 2 platform using the QUARC Real-Time Control Software [28] that is licensed by Quanser and integrated within Simulink (MathWorks Inc.). The QUARC version used is the 4.2.3781 (2022) QUARC creates real-time code directly from Simulink-designed controllers and executes it in real-time on the Windows target, enabling closed-loop control. The hardware mainly consists of a desktop computer with processor Intel® Core(TM) i3-4160 CPU @3.60GHz and the real-time target, the Quanser Aero 2, as illustrated in Fig. 14. A USB communication is used.

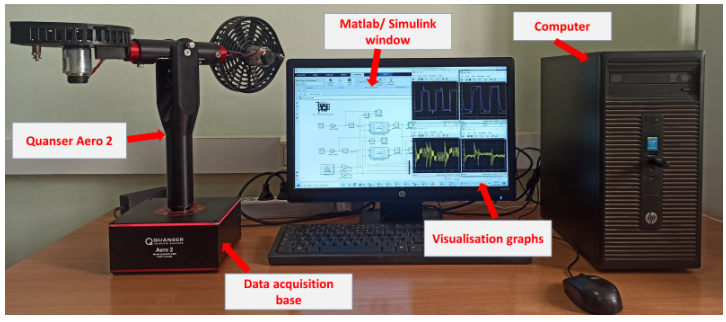

Fig. 14. Hardware laboratory setup

This section presents the experimental results of implementing PID, Fuzzy PID, and ANFIS controllers on the Quanser Aero 2 helicopter. We follow the same simulation procedure to evaluate the three controllers' control performance

and robustness in achieving real-time trajectory tracking. Gains of the conventional PID are kept the same as those used during numerical simulations. Initial conditions are $\theta_0 = 0$ and $\psi_0 = 0$. The desired trajectories for pitch and yaw are chosen as square waves, similar to simulation experiments.

5.1. Case 1: Implementation results without disturbance

At first, we implemented the PID, Fuzzy PID, and ANFIS controllers on the Quanser Aero 2 helicopter without introducing disturbances. Both pitch and yaw motions are recorded and subsequently displayed. Fig. 15 and Fig. 16 illustrate trajectory tracking and tracking errors between desired and measured signals. The initial evaluation without disturbances indicates that all three controllers can effectively track the desired trajectories. The PID controller exhibits the closest tracking for pitch motion, while the Fuzzy PID controller demonstrates superior performance for yaw motion. The ANFIS controller, while still achieving satisfactory tracking, shows slight oscillations around the desired trajectory in both pitch and yaw motions.

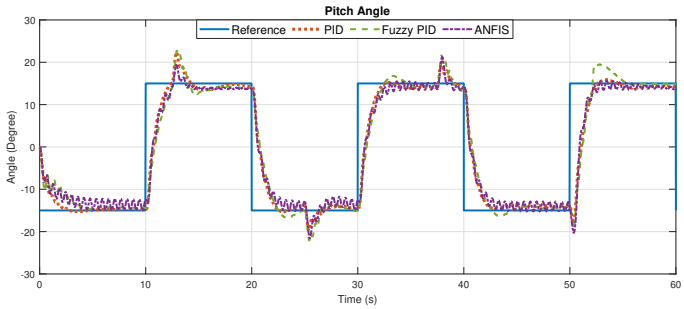

(a) Pitch trajectory tracking hardware result

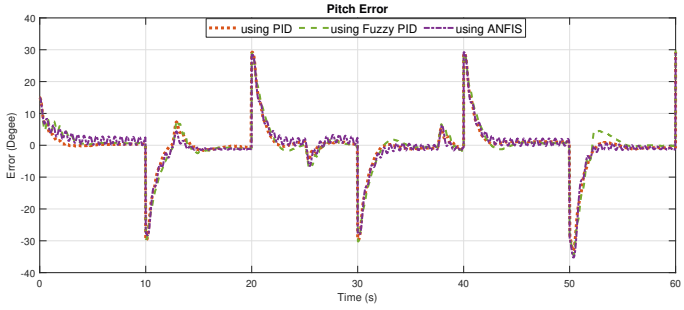

(b) Pitch tracking error hardware

Fig. 15. Hardware response of pitch trajectory tracking: undisturbed Aero 2 system

Fig. 17 and Fig. 18 present the input voltages applied to the pitch and yaw axes to achieve the desired trajectory tracking. These figures reveal that the three controller's input signals remain within the saturation limits for both axes. The

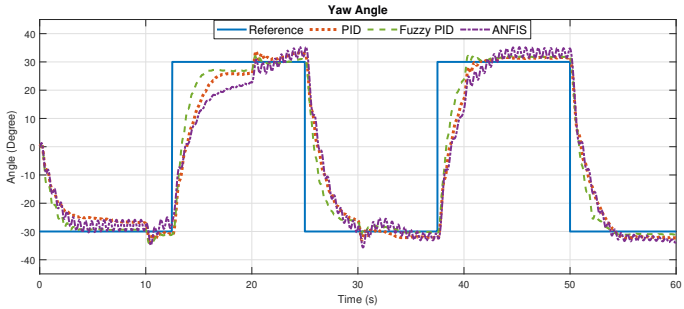

(a) Yaw trajectory tracking hardware result

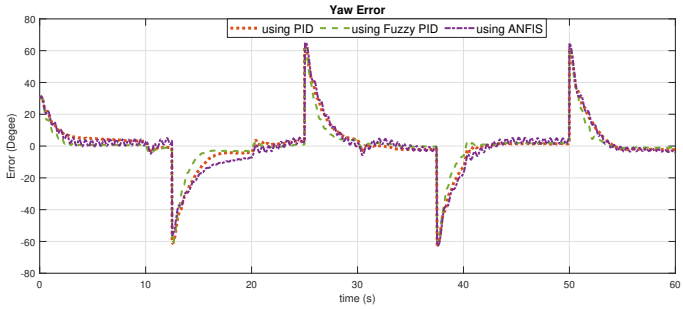

(b) Yaw tracking error hardware

Fig. 16. Hardware response of yaw trajectory tracking: undisturbed Aero 2 system

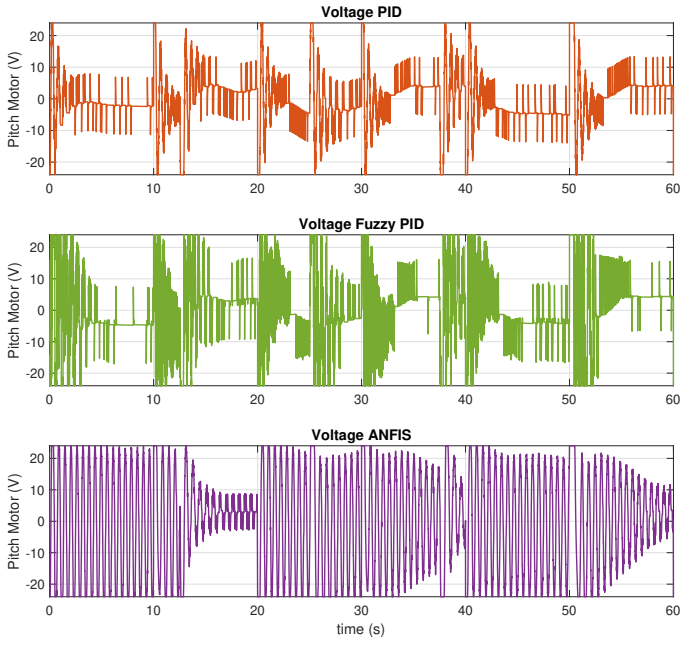

Fig. 17. Hardware control performance for the pitch without disturbance

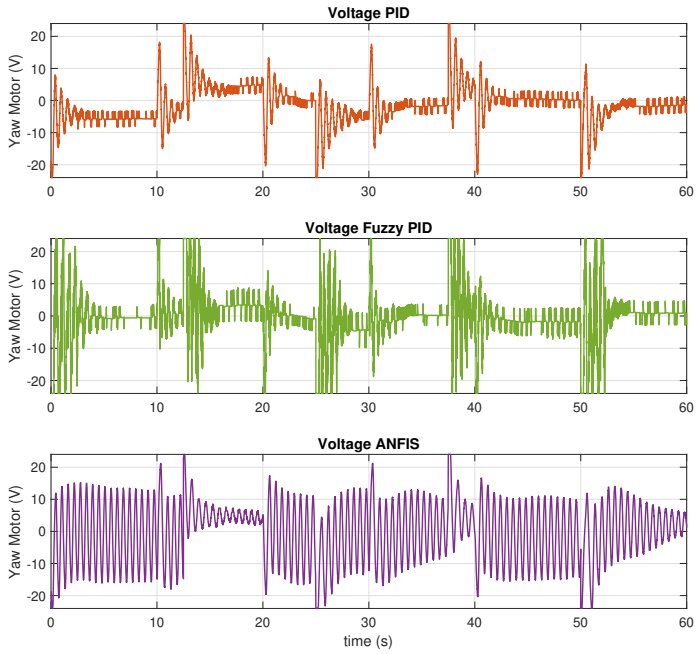

Fig. 18. Hardware control performance for the yaw without disturbance

PID controller's input signal is less likely to reach saturation as compared to the other controllers. In contrast, the ANFIS controller exhibits input signals that consistently reach saturation levels, suggesting a more aggressive control approach. This observation aligns with the slightly oscillatory nature of the ANFIS controller's response seen in the trajectory tracking figures.

5.2. Case 2: Implementation results with matched disturbance

To experimentally assess the robustness of the PID, Fuzzy PID, and ANFIS controllers in the presence of cross-coupling, uncertainties, and matched disturbances, we introduced a non-vanishing band-limited white noise signal as a matched disturbance to the torque input channels of the pitch and yaw motors, respectively. This disturbance is introduced to mimic known disturbances that might affect aerospace applications such as wind gusts or changes in the aircraft's mass distribution during flight.

The obtained hardware responses are recorded and displayed in Fig. 19 and Fig. 20. It is observed that despite the presence of uncertainties, cross-coupling, and matched disturbance, all three controllers reach and track effective trajectory tracking. The PID controller exhibits a smoother response for the pitch motion with less overshoot compared to the Fuzzy PID and ANFIS controllers. However, for the yaw motion, the Fuzzy PID controller outperforms the PID and ANFIS controllers

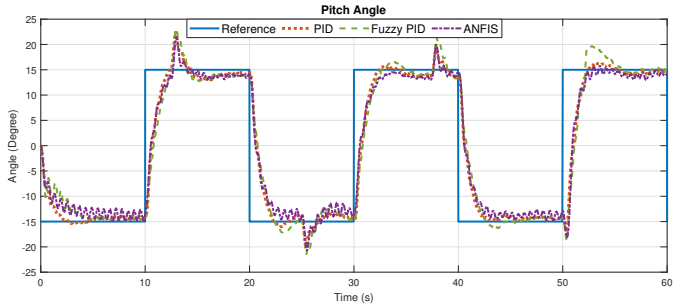

(a) Pitch trajectory tracking hardware result

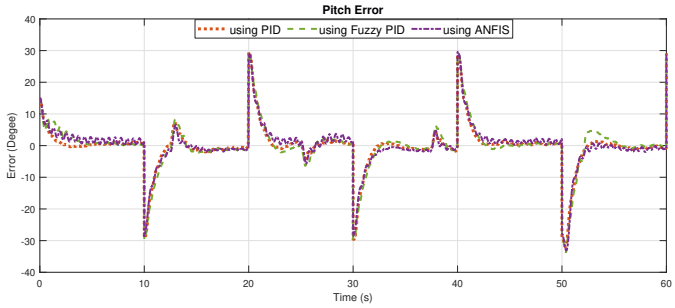

(b) Pitch tracking error hardware

Fig. 19. Hardware response of pitch trajectory tracking with matched disturbances

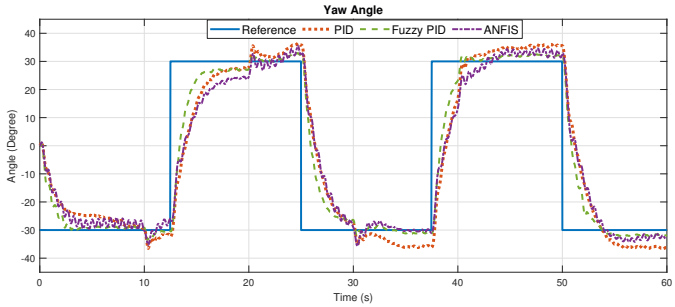

(a) Yaw trajectory tracking hardware result

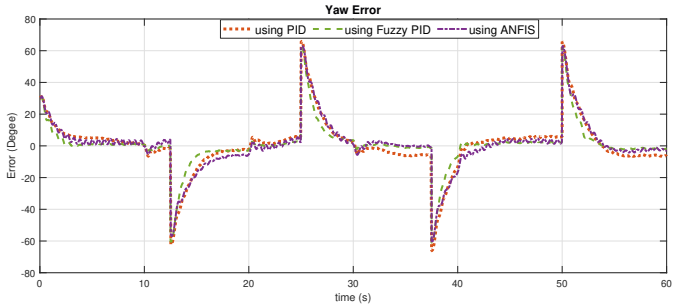

(b) Yaw tracking error hardware

Fig. 20. Hardware response of yaw trajectory tracking with matched disturbances

in terms of tracking accuracy and overshoot minimization. The ANFIS controller, while still achieving satisfactory tracking, presents slight oscillations around the desired trajectories for both axes.

Fig. 21 and Fig. 22 present the input voltages applied to the pitch and yaw motors to achieve trajectory tracking in the presence of cross-coupling, uncertainties, and matched disturbances. These figures reveal that the control signals become significantly more noisy compared to the disturbance-free case. Yet, the three controllers successfully achieve trajectory tracking. It is observed that the ANFIS controller's input signal exhibits a higher degree of saturation compared to the PID and Fuzzy PID controllers. The increased noise levels and control effort highlight the challenges of maintaining precise tracking in the presence of external perturbations. The controllers need to balance tracking accuracy with robustness to disturbances and cross-coupling, while also considering the limitations of the actuators.

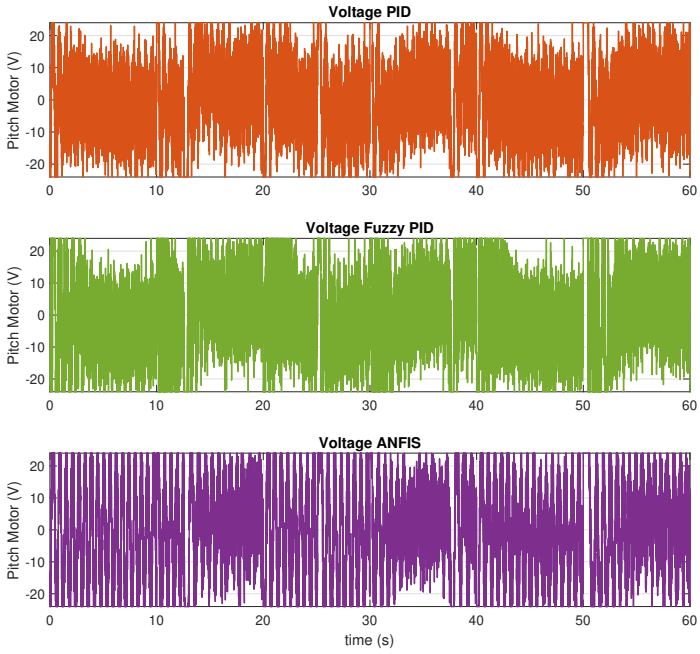

Fig. 21. Hardware control performance for the pitch under matched disturbance

5.3. Comparison of hardware implementation results

Following a similar quantitative evaluation procedure to compare the controllers' response from a real-time hardware implementation viewpoint on the Quanser Aero 2 helicopter, we analyze the obtained results in terms of RMSE, peak value, ISE, IAE, and ITAE as presented in Table. 7 and Table. 8.

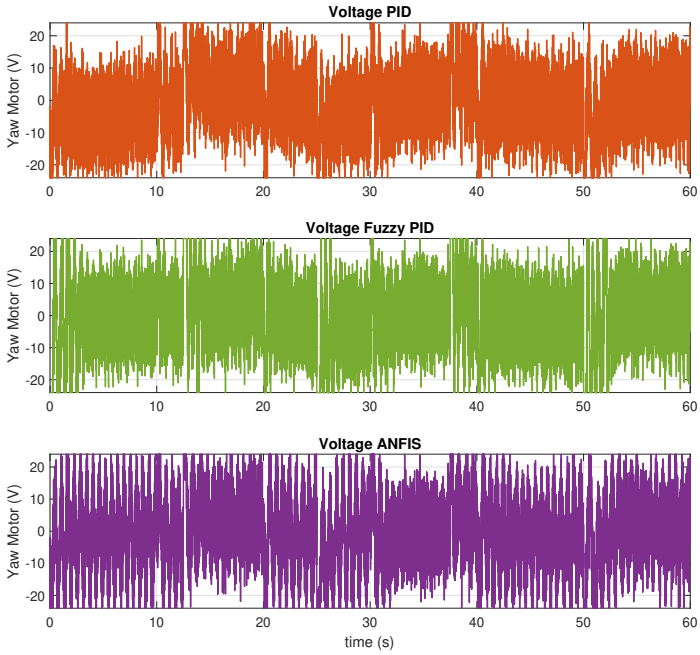

Fig. 22. Hardware control performance for the yaw under matched disturbance

Analyzing the pitch motion, the PID controller demonstrates the lowest RMSE, ISE, IAE, and ITAE values for both undisturbed and disturbed systems, followed by the ANFIS controller and then the Fuzzy PID controller, indicating better tracking accuracy and minimizing overall error accumulation. In terms of peak value, the ANFIS controller shows the smallest peak value which represents a minimal overshoot.

For the yaw motion, the Fuzzy PID controller comes out as the most effective controller, achieving the lowest peak value, RMSE, ISE, IAE, and ITAE values for both undisturbed and disturbed systems. The ANFIS controller follows closely behind, then the PID controller. These results follow the observations made from the trajectory tracking graphs.

Table 7. Hardware response comparison for pitch axis

	Without disturbance			Disturbed model		
Metric	PID	Fuzzy PID	ANFIS	PID	Fuzzy PID	ANFIS
RMSE	**6.910**	7.472	7.115	**6.769**	7.401	6.839
Peak Value (°)	22.37	22.75	**21.25**	23.38	22.12	**21.50**
ISE ($\times 10^4$)	**0.286**	0.334	0.303	**0.275**	0.328	0.280
IAE ($\times 10^4$)	**188.1**	226.7	215.9	**184.3**	227.8	214.7
ITAE ($\times 10^4$)	**0.572**	0.656	0.619	**0.546**	0.662	0.625

Table 8. Hardware response comparison for yaw axis

	Without disturbance			Disturbed model		
Metric	PID	Fuzzy PID	ANFIS	PID	Fuzzy PID	ANFIS
RMSE	15.28	**13.26**	15.92	16.46	**13.50**	15.78
Peak Value (°)	33.84	**32.17**	35.33	36.47	**32.96**	35.51
ISE ($\times 10^4$)	1.401	**1.056**	1.521	1.626	**1.093**	1.494
IAE ($\times 10^4$)	503.3	**365.4**	547.6	594.6	**380.7**	536.0
ITAE ($\times 10^4$)	1.383	**1.050**	1.566	1.781	**1.113**	1.544

6. Discussion

The analysis of the obtained results of this study revealed significant differences in control performance between simulated and hardware implementations of trajectory tracking tasks for Quanser Aero 2 helicopter. In simulations, the ANFIS controller exhibited superior pitch control under both disturbed and undisturbed conditions, as demonstrated by the smallest RMSE, ISE, IAE and ITAE values. However, during hardware validation, the ANFIS control yielded inferior pitch control results compared to the simulations with small oscillations around desired trajectories. In contrast, the Fuzzy PID controller maintained its enhanced yaw control capabilities across both simulated and hardware environments, suggesting robustness to unmodeled dynamics and uncertainties inherent to real-world testing. These differences emphasize the importance of validating control systems using hardware, as simulations alone may not adequately capture factors influencing closed-loop performance. Hardware constraints or unmodeled dynamics may be responsible for ANFIS control's unexpected decline in performance. Additionally, PID's simpler structure may have granted it an advantage in adapting to real-world complexities. Further investigation into specific factors influencing these performances in achieving accurate trajectory tracking is essential for refining simulations and ensuring effective controller design for real-world deployment.

7. Conclusion

This study provided a comprehensive evaluation of PID, Fuzzy PID, and ANFIS controllers for robust trajectory tracking of the Quanser Aero 2 2-DOF helicopter system under parametric uncertainties, unmodeled dynamics, cross-coupling, and matched disturbances. The controllers' performance was rigorously assessed through simulations and real-time hardware experiments. Simulation results highlighted the controllers' robustness and adaptability under different disturbance scenarios. Hardware experiments validated these results, revealing factors influencing real-world closed-loop performance. Quantitative metrics, including RMSE, ISE, IAE, ITAE, and peak values, allowed rigorous analysis, underscoring

the trade-off between tracking accuracy and control effort. Throughout this analysis, we conclude that the Fuzzy PID controller excels in handling non-linearities and uncertainties, particularly for yaw control, but faces challenges in rule base design and computational efficiency. On the other hand, the ANFIS controller offers superior adaptation to changing dynamics and improved trajectory tracking, yet is limited by its dependence on quality training data and potential overfitting. This suggests the development of a hybrid controller combining PID, Fuzzy PID, and ANFIS techniques in future work, as well as an adaptive tuning method for Fuzzy PID and ANFIS controllers to optimize performance in real-time under varying conditions.

References

[1] S. Iqbal. A study on UAV operating system security and future research challenges. In *2021 IEEE 11th Annual Computing and Communication Workshop and Conference (CCWC)*, pages 0759–0765, Las Vegas, USA, 2021. doi: 10.1109/CCWC51732.2021.9376151.

[2] X. Li and A.V. Savkin. Networked unmanned aerial vehicles for surveillance and monitoring: A survey. *Future Internet*, 13(7):174, 2021. doi: 10.3390/fi13070174.

[3] A.W.N. Ibrahim, P.W. Ching, G.L.G Seet, W.S.M. Lau, and W. Czajewski. Moving objects detection and tracking framework for UAV-based surveillance. In *2010 Fourth Pacific-Rim Symposium on Image and Video Technology*, pages 456–461, Singapore, 2010. doi: 10.1109/PSIVT.2010.83.

[4] Z. Zhao, J. Zhang, Z. Liu, C. Mu, and K.-S. Hong. Adaptive neural network control of an uncertain 2-DOF helicopter with unknown backlash-like hysteresis and output constraints. *IEEE Transactions on Neural Networks and Learning Systems*, 34(12):10018–10027, 2023. doi: 10.1109/TNNLS.2022.3163572.

[5] M.H. Khalesi, H. Salarieh, and M.S. Foumani. System identification and robust attitude control of an unmanned helicopter using novel low-cost flight control system. *Proceedings of the Institution of Mechanical Engineers, Part I: Journal of Systems and Control Engineering*, 234(5):634–645, 2020. doi: 10.1177/0959651819869718.

[6] C.K. Verginis, C.P. Bechlioulis, A.G. Soldatos, and D. Tsipianitis. Robust trajectory tracking control for uncertain 3-DOF helicopters with prescribed performance. *IEEE/ASME Transactions on Mechatronics*, 27(5):3559–3569, 2022. doi: 10.1109/TMECH.2021.3136046.

[7] R. Fellag, M. Guiatni, M. Hamerlain, and N. Achour. Robust continuous third-order finite time sliding mode controllers for exoskeleton robot. *Archive of Mechanical Engineering*, 68(4):395–414, 2021. doi: 10.24425/ame.2021.138399.

[8] M. Raghappriya and S. Kanthalakshmi. Pitch and yaw motion control of 2 DOF helicopter subjected to faults using sliding-mode control. *Archives of Control Sciences*, 32(2):359–381, 2022. doi: 10.24425/acs.2022.141716.

[9] B. Godbolt, N.I. Vitzilaios, and A.F. Lynch. Experimental validation of a helicopter autopilot design using model-based PID control. *Journal of Intelligent & Robotic Systems*, 70:385–399, 2013. doi: 10.1007/s10846-012-9720-7.

[10] Y. Niu, X. Jin, J. Li, G. Ji, and K. Hu. The development tendency of artificial intelligence in command and control: a brief survey. *Journal of Physics: Conference Series*, 1883:012152, 2021. doi: 10.1088/1742-6596/1883/1/012152.

[11] O.F. Lutfy, M.S.B. Noor, M.H. Marhaban, and K.A. Abbas. A genetically trained adaptive neuro-fuzzy inference system network utilized as a proportional-integral-derivative-like feedback controller for non-linear systems. *Proceedings of the Institution of Mechanical Engineers, Part I: Journal of Systems and Control Engineering*, 223(3):309–321, 2009. doi: 10.1243/09596518JSCE683.

[12] L.A. Zadeh. Fuzzy sets. *Information and Control*, 8(3):338–353, 1965. doi: 10.1016/S0019-9958(65)90241-X.

[13] A. Chaudhary and B. Bhushan. Trajectory tracking of a 2-DOF helicopter system using fuzzy controller approach. In *2021 International Conference on Emerging Techniques in Computational Intelligence (ICETCI)*, pages 159–164, Hyderabad, India, 2021. doi: 10.1109/ICETCI51973.2021.9574049.

[14] M. Jahed and M. Farrokhi. Robust adaptive fuzzy control of twin rotor MIMO system. *Soft Computing*, 17:1847–1860, 2013. doi: 10.1007/s00500-013-1026-6.

[15] S. Zeghlache, K. Kara, and D. Saigaa. Type-2 fuzzy logic control of a 2-DOF helicopter (TRMS system). *Open Engineering*, 4(3):303–315, 2014. doi: 10.2478/s13531-013-0157-y.

[16] O. Saleem and J. Iqbal. Fuzzy-immune-regulated adaptive degree-of-stability LQR for a self-balancing robotic mechanism: design and HIL realization. *IEEE Robotics and Automation Letters*, 8(8):4577–4584, 2023. doi: 10.1109/LRA.2023.3286176.

[17] Y. Mehmood, J. Aslam, N. Ullah, A.A. Alsheikhy, E.U. Din, and J. Iqbal. Robust fuzzy sliding mode controller for a skid-steered vehicle subjected to friction variations. *PLoS One*, 16(11):e0258909, 2021. doi: 10.1371/journal.pone.0258909.

[18] S. Sadala, B. Patre, and D. Ginoya. A new continuous integral sliding mode control algorithm for inverted pendulum and 2-DOF helicopter nonlinear systems: Theory and experiment. *Proceedings of the Institution of Mechanical Engineers, Part I: Journal of Systems and Control Engineering*, 236(3):518–530, 2022. doi: 10.1177/09596518211048022.

[19] R. Fellag, M. Guiatni, M. Hamerlain, and N. Achour. Adaptive finite-time robust sliding mode controller for upper limb exoskeleton robot. In *2022 19th International Multi-Conference on Systems, Signals and Devices (SSD)*, pages 1255–1260, Setif, Algeria, 2022. doi: 10.1109/SSD54932.2022.9955820.

[20] A.H. Zaeri, S.B. Mohd-Noor, M.M. Isa, F.S. Taip, and A.E. Marnani. Disturbance rejection for a 2-DOF nonlinear helicopter model by using MIMO fuzzy sliding mode control with boundary layer. In *2012 Third International Conference on Intelligent Systems Modelling and Simulation*, pages 411–416, Kota Kinabalu, Malaysia, 2012. doi: 10.1109/ISMS.2012.129.

[21] O. Saleem, K.R. Ahmad, and J. Iqbal. Fuzzy-augmented model reference adaptive PID control law design for robust voltage regulation in DC–DC buck converters. *Mathematics*, 12(12):1893, 2024. doi: 10.3390/math12121893.

[22] M. Pelc. Self-tuning run-time reconfigurable PID controller. *Archives of Control Sciences*, 21(2):189–205, 2011. doi: 10.2478/v10170-010-0039-y.

[23] R. Singh and B. Bhushan. Adaptive neuro-fuzzy-PID and fuzzy-PID-based controller design for helicopter system. In *Applications of Computing, Automation and Wireless Systems in Electrical Engineering: Proceedings of MARC 2018*, pages 281–293. Singapore, 2019. doi: 10.1007/978-981-13-6772-4_25.

[24] M.A. Khanesar and E. Kayacan. Controlling the pitch and yaw angles of a 2-DOF helicopter using interval type-2 fuzzy neural networks. In: Yu, X., Önder Efe, M. (eds) *Recent Advances in Sliding Modes: From Control to Intelligent Mechatronics*, pages 349–370, Springer, 2015. doi: 10.1007/978-3-319-18290-2_17.

[25] A.C. Aras and O. Kaynak. Trajectory tracking of a 2-DOF helicopter system using neuro-fuzzy system with parameterized conjunctors. In *2014 IEEE/ASME International Conference on Advanced Intelligent Mechatronics*, pages 322–326, Besacon, France, 2014. doi: 10.1109/AIM.2014.6878099.

[26] J.-S.R. Jang. ANFIS: adaptive-network-based fuzzy inference system. *IEEE Transactions on Systems, Man, and Cybernetics*, 23(3):665–685, 1993. doi: 10.1109/21.256541.

[27] M. Öztürk and İ. Özkol. Comparison of self-tuned neuro-fuzzy controllers on 2 DOF helicopter: an application. *SN Applied Sciences*, 3(1):124, 2021. doi: 10.1007/s42452-020-03984-5.

[28] Quanser. Quarc real-time control software. https://www.quanser.com/products/quarc-real-time-control-software/#overview, 2022. [Accessed 18-09-2024].

[29] Quanser. Aero 2 : Reconfigurable dual-rotor aerospace experiment for controls education and research. https://www.quanser.com/products/aero-2/, 2022. [Accessed 18-09-2024].

[30] Quanser. *Quanser Aero 2 Laboratory guide*. Quanser, 2022.

[31] R. Fellag and M. Belhocine. 2-DOF helicopter control via state feedback and full/reduced-order observers. In *2024 2nd International Conference on Electrical Engineering and Automatic Control (ICEEAC)*, pages 1–6, Setif, Algeria, 2024. doi: 10.1109/ICEEAC61226.2024.10576208.

[32] Y.-C. Ho. Review of book: J.S.R. Jang, C.T. Sun, and E. Mizutani. *Neuro-fuzzy and soft computing-a computational approach to learning and machine intelligence*. *IEEE Transactions on Automatic Control*, 42(10):1482–1484, 1997.

[33] F. Liu, H. Wang, Q. Shi, H. Wang, M. Zhang, and H. Zhao. Comparison of an ANFIS and fuzzy PID control model for performance in a two-axis inertial stabilized platform. *IEEE Access*, 5:12951–12962, 2017. doi: 10.1109/ACCESS.2017.2723541.

[34] Inc The MathWorks. Neuro-Adaptive Learning and ANFIS – MATLAB & Simulink – mathworks.com. https://www.mathworks.com/help/fuzzy/neuro-adaptive-learning-and-anfis.html, 2023. [Accessed 18-09-2024].